HHS Public Access

Author manuscript

Neuroimage. Author manuscript; available in PMC 2022 August 01.

Published in final edited form as:

Neuroimage. 2022 August 01; 256: 119274. doi:10.1016/j.neuroimage.2022.119274.

Dynamic trajectories of connectome state transitions are heritable

Suhnyoung Jun[a,b],

Thomas H. Alderson[a],

Andre Altmann[c],

Sepideh Sadaghiani[a,b,d,*]

[a]Beckman Institute for Advanced Science and Technology, University of Illinois at Urbana-Champaign, Urbana, Illinois, 618201

[b]Psychology Department, University of Illinois at Urbana-Champaign, Urbana, Illinois 61801

[c]Centre for Medical Image Computing (CMIC), Department of Medical Physics, University College London, London, UK

[d]Neuroscience Program, University of Illinois at Urbana-Champaign, Urbana, Illinois 61801

Abstract

The brain's functional connectome is dynamic, constantly reconfiguring in an individual-specific manner. However, which characteristics of such reconfigurations are subject to genetic effects, and to what extent, is largely unknown. Here, we identified heritable dynamic features, quantified their heritability, and determined their association with cognitive phenotypes. In resting-state fMRI, we obtained multivariate features, each describing a temporal or spatial characteristic of connectome dynamics jointly over a set of connectome states. We found strong evidence for heritability of temporal features, particularly, Fractional Occupancy (FO) and Transition Probability (TP), representing the duration spent in each connectivity configuration and the frequency of shifting between configurations, respectively. These effects were robust against methodological choices of number of states and global signal regression. Genetic effects explained a substantial proportion of phenotypic variance of these features (h^2 = 0.39, 95% CI = [.24,.54] for FO; h^2 = *0*. 43, 95% CI = [.29,.57] for TP). Moreover, these temporal phenotypes were associated with cognitive performance. Contrarily, we found no robust evidence for heritability of spatial features of the dynamic states (i.e., states' Modularity and connectivity pattern). Genetic effects may therefore primarily contribute to how the connectome *transitions* across states, rather than the precise spatial

*Corresponding author. sepideh@illinois.edu (S. Sadaghiani).

Competing Interest Statement

The authors declare no competing interest.

Credit authorship contribution statement

Suhnyoung Jun: Formal analysis, Visualization, Writing – original draft, Writing – review & editing. **Thomas H. Alderson**: Methodology, Writing – original draft. **Andre Altmann**: Methodology, Writing – review & editing. **Sepideh Sadaghiani**: Supervision, Conceptualization, Writing – original draft, Writing – review & editing, Project administration.

Supplementary materials

Supplementary material associated with this article can be found, in the online version, at doi: 10.1016/j.neuroimage.2022.119274.

instantiation of the states in individuals. In sum, genetic effects impact the dynamic trajectory of state transitions (captured by FO and TP), and such temporal features may act as endophenotypes for cognitive abilities.

Keywords

Dynamic functional connectivity; Heritability; Variance component modeling; Twin study; Hidden markov modeling

Introduction

Inter-individual variability in the time-averaged (static) functional connectivity architecture of the human brain is subject-specific and predictive of cognitive abilities (Finn et al., 2015; Jalbrzikowski et al., 2020; Ousdal et al., 2020; Rosenberg et al., 2016; Gratton et al., 2018). With the increasing availability of large-sample fMRI datasets, significant genetic contributions to this *static* large-scale connectome architecture have been established. Specifically, individual connections (region-pairs) and networks of the functional connectome have been identified as heritable (Ge et al., 2017; Reineberg et al., 2020; Glahn et al., 2010; Colclough et al., 2017). Moreover, topological properties of the static connectome, such as the modular organization, have been shown to con-stitute heritable subject-specific traits linked to behavioral and cognitive characteristics (Liu et al., 2019; Sinclair et al., 2015).

However, the static architecture captures only part of the functionally significant properties of the connectome. In fact, the functional connectome as measured by fMRI spontaneously exhibits flexible reconfigurations over the course of seconds to minutes (Lurie et al., 2020; Keilholz 2014). These reconfigurations can be described as changes in connectivity strength between specific sets of brain region-pairs, forming recurrent connectome states. Such functional connectome states hold great significance as their time-varying (dynamic) characteristics measured during task-free resting state have been linked to behavior and cognition (Eichenbaum et al., 2020; Vidaurre et al., 2017).

Because some of the same behavioral and cognitive features linked to connectome dynamics are also heritable (Han and Adolphs 2020), the possibility emerges that the behaviorally relevant connectome dynamics may themselves be heritable. A prior study provides some support for this exciting possibility by demonstrating heritability of the ratio of time spent across two “meta-states ” and their association with cognitive abilities (Vidaurre et al., 2017). However, the magnitude of heritability of such dynamic features, i.e.,% variance of the dynamic features explained by genetic effects, was not assessed. Another informative study has provided estimation of heritability magnitude for the variance and mean of a connection-wise dynamic connectivity measure (Barber et al., 2021). However, the measure was assessed separately for each pair of canonical intrinsic connectivity networks (ICNs) rather than the comprehensive architecture of connectome states, and the link between the dynamic features and cognition was not investigated. Here, we argue that future advances in genetics neuroimaging of connectome dynamics and its translational potential are contingent upon identifying which dynamic features are heritable and linked to behavior. Therefore,

in the following we focus on a set of dynamic connectome features that have been most commonly reported as behaviorally relevant. This hypothesis-driven approach allows us to home in on a select subset among the numerous possible network features.

Particular *temporal* features of connectome dynamics, such as durations and rates of states, or the probability of transitions among states, have been shown to be behaviorally relevant (Nomi et al., 2017). Specifically, the proportion of the total recording time spent in each connectome state (Fractional Occupancy) and the probability to transition between specific pairs of discrete states (Transition Probability) have been linked to behavior (Eichenbaum et al., 2020; Vidaurre et al., 2017). These temporal features are different from the above-described spatial features in that they define the state sequence, or the *trajectory* of the connectome through state space, rather than the states' spatial pattern of FC strength. In fact, the matrix of Transition Probability values between all possible state-pairs fully characterizes connectome transitions.

Beyond these temporal attributes of connectome reorganization, an often-reported observation is that dynamic changes in the *spatial* features of the connectome shape behavior. By spatial features, we refer to patterns of connection strength and ensuing topological characteristics of connectome states. Indeed, spontaneous changes in the functional connectivity pattern of specific sets of connections have been linked to a wide range of cognitive processes from perception to higher-order control (Sadaghiani et al., 2015; Thompson et al., 2013; Douw et al., 2016; Hellyer et al., 2014; Vatansever et al., 2017). Beyond specific sets of connections, global topological properties of the connectome's graph measure the spatial connectome pattern of *all* connections in a wholistic manner (Rubinov and Sporns 2010). Modularity is the topological feature whose dynamics (Betzel et al., 2016) are most commonly associated with various behaviors (J. R. Cohen and D'Esposito 2016; Finc et al., 2017; Sadaghiani et al., 2015; Shine et al., 2016). Modularity quantifies the balance between segregation (prioritizing processing within specialized networks) and integration (combining specialized information from various networks) (Shine and Poldrack 2018). While modularity of the *static* connectome was found to be heritable (Sinclair et al., 2015), genetic contributions to the behaviorally-relevant *time-varying dynamics* of Modularity across connectome states have not been assessed.

Based on the preceding evidence for behavioral relevance, we chose to investigate two dynamic *temporal* features and two dynamic *spatial* features. Specifically, the temporal features comprised Fractional Occupancy and Transition Probability. The two *spatial* features included the time-varying connectivity strength ($FC_{Time\text{-}Varying}$) of the set of connections exhibiting the strongest dynamic changes across states (cluster of connections selected in a data-driven manner; Zalesky et al., 2010), and time-varying Modularity ($Modularity_{Time\text{-}Varying}$). We sought to answer (i) whether the hypothesis-driven temporal and spatial features of connectome dynamics are heritable; (ii) whether such heritability emerges from *multivariate* phenotypes jointly encompassing all connectome states or contrarily as phenotypes of individual states; (iii) how much of the phenotypic variance of the dynamic connectome features can be accounted for by genetic influence; and (iv) how much of the variance in heritable dynamic connectome features is associated with the individual variability in cognitive domains. To address these questions, we extracted discrete

brain states from resting-state fMRI data acquired from the Human Connectome Project (Smith et al., 2013), including monozygotic and dizygotic twin pairs, non-twin sibling pairs, and pairs of unrelated individuals, estimated their dynamic features, fitted quantitative genetic models to the features, and quantified their association with cognition.

2. Materials and methods

Fig. 1 is a schematic representation of the overall approach and analysis subsections. Because neuroimaging data processing inevitably involves numerous decision points, we provide reasoning for our choices, and further include supplementary results for several alternative choices where appropriate (see Supplementary Information).

2.1. Neuroimaging and behavior dataset

We used the Washington University-University of Minnesota (WUMinn) consortium of the Human Connectome Project (HCP) S1200 release (Van Essen et al. 2013). Participants were recruited, and informed consent was acquired by the WU-Minn HCP consortium according to procedures approved by the Washington University IRB (Glasser et al., 2013). For details of the HCP data collection protocol and cognitive measures, see (Smith et al., 2013; Van Essen et al. 2013) and (Barch et al., 2013), respectively.

From the pool of all 1003 healthy adult subjects (aged 22–37 y, 534 females) with four complete resting-state fMRI runs (4800 total timepoints) we investigated 120 monozygotic (MZ) twin pairs, 65 sex-matched dizygotic (DZ) twin pairs, 96 sex-matched non-twin (NT) sibling pairs, and 62 pairs of sex-matched unrelated individuals. Note that all pairs are uniquely defined so that none of the subjects overlap between groups to avoid dependencies across members of families with > 2 subjects. All 1003 subjects entered HMM estimation of discrete connectome states, while 686 subjects (as described in the pairs above) entered heritability analysis. We included all 14 cognitive measures, which are summary scores for either a cognitive task or a questionnaire, under the cognition domain provided by the HCP (see Table S1 for more detailed description for each variable, and Fig. S6A for their phenotypic correlation structure). The measures were z-score normalized to zero mean and unit variance. Of 1003 subjects, 997 subjects had complete data for the 14 cognitive variables measuring cognitive performance and entered canonical correlation analysis (CCA).

2.2. Neuroimaging data preprocessing

All imaging data were acquired on a customized Siemens 3T Skyra at Washington University in St. Louis using a multi-band sequence. Each 15-minute resting-state fMRI run was minimally preprocessed (Glasser et al., 2013) using tools from FSL (Jenkinson et al., 2012) and Freesurfer (Fischl 2012), and had artifacts removed using ICA + FIX (Griffanti et al., 2014; Salimi-Khorshidi et al., 2014). Preprocessing following the pipeline of Smith et al. (Smith et al., 2013, et al. 2013). Inter-subject registration of cerebral cortex was carried out using arealfeature-based alignment and the Multimodal Surface Matching algorithm (‘MSMAll’) (Glasser et al., 2016; Robinson et al., 2014).

2.3. Parcellation

The HCP team has previously parcellated the neuroimaging data with ICA in FSL using various model orders of 25, 50, 100, 200, and 300 independent components. Specifically, for group-ICA, each dataset was temporally demeaned and variance normalized (Beckmann and Smith 2004). HCP provides averaged BOLD time-series for regions of these group-ICA-based parcellations. We used the time-series both with and without global signal regression (GSR), reasoning that robust heritability effects would be evident regardless of the choice of GSR/non-GSR.

Among the available parcellations, the 300 model order ICA was chosen for this study due to its following advantages: (i) independent components in this parcellation better separate the *individual* brain areas of the intrinsic connectivity networks (ICNs) than the lower model orders; (ii) in this parcellation those independent components with multiple brain regions spatially overlaps with a single ICN, whereas in lower model orders, independent components may overlap with multiple ICNs, making it difficult to consider the BOLD time-series extracted from a given independent component as representing a single ICN.

However, the 300-model order ICA resulted in additional extreme parcellation of the cerebellum and brainstem; 161 out of 300 independent components were identified as either cerebellar or brainstem using Automated Anatomical Labeling (AAL) atlas-based masks, confirmed by visual inspection. Including these regions would underestimate the contribution of canonical ICNs to the dynamic reconfiguration of the connectome, as the cortical and subcortical cerebrum comprises a considerably larger overall volume but fewer independent components than the cerebellum and brainstem. FC reconfigurations among canonical neurocognitive ICNs have been described as key contributors to the behavioral impact of connectome dynamics (Douw et al., 2016; Hellyer et al., 2014; Sadaghiani et al., 2015; Thompson et al., 2013; Vatansever et al., 2017) and thus form the core of our features of interest. Therefore, we focused our investigation on the cerebral ICNs by excluding independent components which fall into the cerebellar/brainstem regions, resulting in a total of 139 out of 300 independent components.

We computed the spatial overlap between each of the 139 independent components and Yeo's canonical neurocognitive ICNs (Yeo et al., 2011) to identify the functional network represented by each independent component. Yeo's 7 ICNs include visual network (VIS), sensory-motor network (SMN), dorsal attention network (DAN), salience/cingulo-opercular network (CON called Ventral Attention by Yeo et al.), limbic network (Limbic), frontoparietal network (FPN), and default mode network (DMN). While Yeo's 7 ICNs are limited to cortical surface maps, the Limbic system is well-known to include core subcortical regions. To add these regions to our Limbic network, we selected the respective independent components that overlapped with an additional subcortical mask from the AAL atlas including the bilateral hippocampus, thalamus, as well caudate, putamen, and pallidum regions that they are heavily connected to (see Fig. S1 for the independent components grouped into the 7 ICNs).

2.4. Hidden markov modeling

We applied a hidden Markov model (HMM) to the minimally preprocessed region-wise BOLD time-series, resulting in K discrete states of whole-brain connectivity, each associated with state-specific timecourse. The HMM assumes that time series data can be described using a finite sequence of a hidden number of states. Each state and its associated time series comprise a unique connectivity pattern that temporally re-occurs over time. Using the HMM-MAR (multivariate autoregressive) toolbox (Vidaurre et al., 2016), discrete connectome states were inferred from region-wise BOLD time-series temporally concatenated across all subjects. Whereas the states are estimated at the grouplevel, each individual has a subject-specific state time course, indicating when a given state is active. For a given K, the best fitting model corresponding to the one with the lowest free energy was selected across five runs (Quinn et al., 2018; Vidaurre et al., 2016; 2018).

HMMs require an *a priori* selection of the number of states, K. Generally, the objective is not to establish a 'correct' number of states but to strike a balance between model complexity and model fit and to identify a number that describes the dataset at a useful granularity (Quinn et al., 2018). Prior HMM studies that have directly compared several K s have identified K s between 3 and 7 as optimal (Stevner et al., 2019; Vidaurre et al., 2016). Therefore, we chose $K = 4$ to fall within this range, and further assessed $K = 6$, reasoning that robust heritability effects would be evident regardless of the specific choice of K (within the optimal range).

2.5. Null model

We demonstrated that the dynamic trajectory of connectome state transitions is not random by generating 50 simulated state time courses of the same length as the original empirical state time courses (Vidaurre et al., 2016). Note that fifty is a rigorous choice compared to previous work (e.g., Vidaurre et al. (Vidaurre et al., 2017) applied four simulations). The surrogate data, simulated using the *simhmmmar* function provided by HMM-MAR toolbox, preserve the static covariance structure of the original data but destroy the precise temporal ordering of states. An HMM inference with $K = 4$ and $K = 6$, respectively, was run on each of 50 surrogate datasets and the dynamic connectome features (Fractional Occupancy, Transition Probability, etc.) at the groupand subject-level were recomputed. We confirmed that the non-random distribution of features over states observed in the original dataset was absent in the surrogate dataset (Fig. S7).

2.6. Deriving multivariate temporal features of the dynamic connectome

HMM-derived estimates provided the *multivariate* temporal features of dynamic connectome that concurrently characterize all states. Specifically, we calculated Fractional Occupancy (the cumulative total time spent in a given state) for each HMM-derived state per subject. Further, the transition probabilities across all state-pairs (Transition Probability matrix) were estimated for each subject. Therefore, the temporal features included Fractional Occupancy ($1 \times K$) and off-diagonals of Transition Probability matrix ($K \times K$) (cf. Fig. 1A).

2.7. Deriving multivariate spatial features of the dynamic connectome

As a core global topological characteristic, Newman's Modularity (Newman 2006) was estimated separately for each of the HMM-derived connectome states. Modularity quantified the level of segregation of each connectome state into modules (Brain Connectivity Toolbox (Rubinov and Sporns 2010)), where the modular partition was configured to comprise the canonical ICNs (Yeo et al., 2011). The Modularity value for the K states were then combined into a K-dimensional vector constituting the multivariate feature for heritability analysis.

Our second spatial feature was selected in a maximally data-driven manner. Specifically, we adopted the network-based statistics (NBS) approach (Zalesky et al., 2010) to identify clusters of connections that are significantly different across discrete connectome states. NBS is a non-parametric method that deals with the multiple comparisons problem (multitude of connections) on a graph by identifying the largest connected sub-component (cluster) in topological space while controlling the family-wise error rate (FWER). More specifically, we first performed mass univariate F-testing across four connectome states, adjusting for age and head motion, independently across every connection within the connectome. Importantly, F tests were performed on absolute values for all connections to focus on the strength of connections, regardless of their connectivity direction. As a result, each connection is endowed with a single test statistic (F value) reflecting the connection's change in connectivity value across K states. Then, the test statistic is thresholded to obtain a set of supra-threshold connections, then identify topological clusters among the set of supra-threshold connections. Since the choice of threshold is arbitrary, we chose a range of thresholds (connection densities) that allow 1% to 5% of all connections to survive. Next, significant sets of connected edges, i.e., clusters, were identified at FWER-corrected P-value ($p < .05$) using permutation testing ($n = 5000$). The permutation constructs an empirical null distribution of the largest connected cluster size by randomly rearranging the correspondence between data points and their labels under the null hypothesis without affecting the test statistic. As a result, for each connection density (1 ~5%), NBS-defined clusters that substantially differ across the connectome states are obtained. Finally, at each density, the FC value was averaged among the connections of the data-driven clusters for each of the K states, then combined into a K-dimensional vector. This vector constitutes the multivariate feature that encapsulates the time-varying FC ($FC_{Time\text{-}Varying}$) of data-driven clusters for heritability analysis. We report results for 5% density in the main manuscript and generalize to the other densities in Table S5.

For exploratory analyses, we further included a more comprehensive set of multivariate (K-dimensional) spatial features. Specifically, we investigated $FC_{Time\text{-}Varying}$ for all pairs of the seven canonical ICNs, including each ICN's connectivity to itself (within-network connectivity). The FC value was averaged among the connections of each ICN pair for each of the K states, then combined into a K-dimensional vector. This vector constitutes the multivariate feature that encapsulates the time-varying FC ($FC_{Time\text{-}Varying}$) of the respective ICN pair for heritability analysis. (Table S6–7).

2.8. Similarity estimation and heritability testing

The multidimensional space for each feature was created by setting the origin point to the average of the given multivariate feature from the 50 surrogate datasets (see null model above). Within the multidimensional space constructed for each of the multivariate features, we estimated the similarity of each multivariate feature based on the Euclidean distance between a given pair of subjects (Colclough et al., 2017). Crucially, this similarity estimation approach preserved the positional relationship between elements in each multivariate variable. We tested if the similarity of each of the multivariate features was dependent on the similarity of the genetic makeup between a given subject pair. Specifically, we used a one-way ANCOVA of the factor sibling status with four levels (i.e., MZ twins, DZ twins, NT siblings, and pairs of unrelated individuals) on the similarity of each of the multivariate features, adjusting for age and head motion similarity between subject pairs. Head motion was quantified as framewise displacement (FD) (Power et al., 2012), once in terms of the multivariate FD pattern across states (used for all analyses reported in the main manuscript, cf. SI Results II for details), and alternatively as FD across the total scan duration (reported in SI Results II).

Further, we examined if heritability of features was driven by the multivariate pattern or by *individual* (i.e., state-by-state) components of the multivariate features. Specifically, we estimated the similarity of each state-specific component of the Fractional Occupancy, $FC_{\text{Time-Varying}}$ of data-driven clusters and Modularity $_{\text{Time-Varying}}$ between a given pair of subjects. Likewise, the similarity of each state-pair component of the Transition Probability matrix was estimated. We used twoway ANCOVAs to examine the effect of sibling status and connectome state on the similarity of individual components of the multivariate features.

2.9. Quantification of heritability

Heritability (h^2) is the proportion of variance of a phenotype explained by genetic variance. We employed a structural equation modeling commonly used in classical twin studies to estimate heritability applied in twin studies. With multiple biological assumptions (Keller and Coventry 2005), including that environment affects MZ and DZ twins equally, the structural equations modeling partitions the phenotypic variance into the three components (A, C, and E) using maximum likelihood methods: additive genetic variance (A; resulting from additive effects of alleles at each contributing locus), common environmental variance (C; resulting from common environmental effects for both members of a twin pair), and random environmental variance (E; resulting from non-shared environmental) (Yashin and Iachine 1995).

The ACE model finds the correlation of univariate phenotypes between twin pairs and requires each subject to have a singular value for each phenotype. To accommodate the multivariate phenotypes to be fitted into the model, we defined an origin point from which the Euclidean distance of each multivariate phenotype will be estimated for each subject (Fig. 1).

This method was implemented in the *R* package *mets* (http://cran.rproject.org/web/packages/mets/index.html), adjusting for age and head motion. Nested models, specifically AE and

CE, were fitted by dropping C or A, respectively. Statistical significance of nested models was assessed by a likelihood ratio test and the fitness of models was tested using the Akaike's Information Criterion (AIC) (Akaike 1987).

2.10. Relating dynamic trajectories of states to cognitive performance

Canonical correlation analysis (CCA) is a multivariate technique that can identify and measure linear relations between two sets of variables (Hotelling 1936). The CCA uses the Rao's approximation approach to test the null hypothesis that each linear relationship (or "mode ") between the U and V canonical variates is zero. As a result, the significance of each mode is estimated. As previously applied to the static connectome and HMM-derived states, we trained CCA on the dimensionality-reduced temporal phenotypes of the connectome dynamics (U canonical variate matrix) and cognitive measures (V canonical variate matrix) (Eichenbaum et al., 2020; Smith et al., 2015; Vidaurre et al., 2017; Tibon et al., 2021). Specifically, the canonical variate U consisted of 16 temporal phenotypes of connectome dynamics (i.e., 4 dimensions from $1 \times K$ Fractional Occupancy and 12 dimensions from the off diagonals of $K \times K$ Transition Probability matrix) and the canonical variate V consisted of 14 cognitive measures. Before applying dimensionality-reduction procedures to each canonical variate, the variables that constitutes the canonical variate were normalized by z-scoring (mean centered to zero and unit variance scaled to one) (Wang et al., 2020).

We performed a principal component analysis (PCA) to 16 dimensions of the canonical variate U to reduce the dimensionality. By retaining principal components of eigenvalues > 1, we identified three principal components, together explaining about 88.27% of the total variance in the temporal features of the dynamic connectome (Fig. S5). For CCA, we used these three principal component coefficients as the U canonical variate.

For canonical variate V, we applied the dimensionality-reduction protocol of the previous study that investigated the heritability of HCP-provided behavioral measures (Han and Adolphs 2020). Specifically, we performed a factor analysis to cluster the cognitive measures into four factors based on maximum likelihood estimates of the factor loadings (Fig. S6C). The number of factors was determined based on the number of principal components having eigenvalues > 1 in a preceding PCA (Fig. S6B). Factors were rotated using Promax oblique rotation because there was no evidence that the factors were orthogonal (Fig. S6A). We also computed factor scores using both regression and Bartlett methods for reliability (since factor scores are indeterminate). These two methods produced two sets of very similar factor scores for the same four factors (see correlation structure between all 8 factor scores in Fig. S6D). For CCA, we used the four factor scores from the regression method as the V canonical variate.

Based on the factor loading matrix showing the variance explained by each cognitive measure on a given factor (Fig. S6C) (Han and Adolphs 2020), we cautiously (and inevitably subjectively) interpret the extracted four factors as follows: factor 1: "Language " (indicated by high positive loadings on language-related cognitive tasks); factor 2: "Impulsivity/self-regulation " (indicated by high positive loadings on delay discounting tasks); factor 3: "Cognitive control " (indicated by high positive loadings on fluid ability measuring tasks);

and factor 4: “Memory ” (indicated by high positive loadings on episodic and working memory tests).

To assess the statistical significance of the discovered modes of covariation, we calculated 10,000 permutations of the rows of U relative to V, respecting the within-participant structure of the data, and recalculated the CCA mode for each permutation in order to build a distribution of canonical variate pair correlation values (Smith et al., 2015). By comparing the outcome from the CCA of the true data to the shuffled data, we found that each mode of covariation discovered with the true data was highly significant ($p < 1/10{,}000$). The contribution of each factor to the given mode was evaluated with post-hoc correlations between the modes and the cognitive factors.

3. Results

Results generated by the analysis procedures (illustrated in Fig. 1) are presented following the progression from Fig. 1A through 1C.

3.1. Discrete connectome states have distinct spatial and temporal profiles

We conceptualize dynamic connectome features as characteristics that describe FC changes between specific discrete connectome states. We extracted discrete connectome states, i.e., whole-brain recurrent connectivity patterns, in a data-driven fashion using hidden Markov modeling (HMM) (Fig. 2A) (Vidaurre et al., 2016). HMMs require an *a priori* selection of the number of states (K), and prior HMM studies that have explored several Ks have identified Ks between 3 and 7 as optimal (Stevner et al., 2019; Vidaurre et al., 2016). Therefore, we chose K *of* 4 to fall within this range, and further assessed K of 6, reasoning that robust heritability effects would be evident regardless of the specific choice of K (within the optimal range). In the following, we show that robust heritability effects are observable in both parameter regimes. Here, we report outcomes for $K = 4$ and replicate results for $K = 6$ in Supplementary Information (SI). Characteristics of connectome states were convergent with prior literature that used similar number of states regardless of state-defining approach (e.g., k-means clustering; Allen et al. 2014; Nomi et al., 2017), most notably a prominent contribution of the visual and somatosensory ICNs to cross-state differences (Fig. 2A).

We directly quantified these cross-state FC differences using Network-Based Statistics (NBS; Zalesky et al., 2010). We applied NBS as a data-driven method to identify connected sets of connections (i.e., clusters) whose FC values differed significantly across connectome states (NBS enables cluster-level correction of multiple comparisons in graph space). Fig. 2C shows the resulting (NBS-corrected) cluster of 473 connections with strong cross-state FC difference (NBS applied at 5% uncorrected connection density out of 9591 total connections). The significant cluster showed large contribution of the visual ICN to the cross-state FC difference. Further, *post hoc* t-tests for FC averaged over all connections of the cluster showed a difference across all pairwise comparisons ($p < .05$); mean FC of the cluster was highest in state 2, followed by state 4, state 1, and lowest in state 3. This pattern of difference across state-pairs was maintained over different connection densities (1% ~ 5%; Fig. S4).

In addition to the strong contribution of the NBS-derived connections to cross-state FC differences, we added exploratory analyses into contributions of all canonical ICNs. Specifically, for each possible pair of canonical ICNs we performed a one-way ANCOVA of the factor state with K levels on FC, adjusting for age and head motion (Ks of 4 and 6 without GSR in Table S2, and with GSR in Table S3). Despite the visual similarity of the stats (Fig. 2A), this exploratory analysis showed that all ICN pairs contributed to FC differences across states.

Beyond the FC of specific sets of connections, we investigated cross-state differences in global topology, specifically Modularity (Newman 2006; Rubinov and Sporns 2010). A one-way ANCOVA of factor state was conducted for Modularity, adjusting for age and head motion. Fig. 2D shows that the connectome states differed significantly with respect to Modularity ($F_{(3, 2532)} = 169.53$, $P = 2.23\text{e-}100$, $\eta^2_p = 0.167$).

Regarding temporal characteristics of the states, an equivalent ANCOVA of factor state was performed on Fractional Occupancy, adjusting for age and head motion. This analysis showed that the cumulative time spent in each state differed across states ($F_{(3, 2738)} = 90.26$, $P = 1.07\text{e-}55$, $\eta^2_p = 0.090$).

In summary, these results confirm that the spontaneous connectivity time courses can be described as non-random sequences of four (or six) discrete connectome states that differ from each other in terms of spatial organization, global topology, and proportion of occurrence.

3.2. Multivariate temporal features of the dynamic connectome are heritable

Heritability was tested for *multivariate* features that concurrently characterize all states. To circumvent the statistical limitations imposed through multiple comparisons, the heritability analysis was confined to a selection of hypothesis-driven phenotypes. Specifically, the multivariate features included Fractional Occupancy ($1 \times K$), Transition Probability matrix ($K \times K$), $FC_{\text{Time-Varying}}$ of data-driven clusters ($1 \times K$), and $\text{Modularity}_{\text{Time-Varying}}$ ($1 \times K$) (cf. Fig. 1A).

We tested the supposition that genetically related subjects had more similar multivariate features than genetically less related subjects. The similarity of each of the multivariate connectome features between a given pair of subjects was quantified as Euclidean distance. Distance values entered a one-way ANCOVA of the factor sibling status with four levels, including monozygotic (MZ) twins, sex-matched dizygotic (DZ) twins, sex-matched non-twin (NT) siblings, and sex-matched pairs of unrelated individuals, adjusted for age and head motion. No subjects overlapped between groups.

We found that temporal features, describing the dynamic trajectory of connectome state transitions, are heritable (Fig. 3A). Specifically, genetically closer subject pairs have more similar Fractional Occupancy ($F_{(3, 337)} = 15.49$, $P^{\dagger} = 7.32\text{e-}9$, $\eta^2_p = 0.121$, where $P^{\dagger}$ is the P value Bonferroni-corrected for four dependent variables) and Transition Probability ($F_{(3, 337)} = 12.00$, $P^{\dagger} = 6.98\text{e-}7$, $\eta^2_p = 0.097$) phenotypes, compared to less genetically-related pairs. This impact of sibling status on temporal features was of consistently large

effect size (partial eta squared (η2p) ~ 0.11; J. Cohen 1988), regardless of global signal regression (GSR) and the chosen number of states (see SI Results I, Fig. S2). No effect of sibling status was observed in surrogate data lacking time-varying dynamics but with preserved static covariance structure (Fractional Occupancy $F_{(3, 337)} = 0.66$, $P^{\dagger} = 1$, $\eta^2_p = 0.006$, and Transition Probability $F_{(3, 337)} = 0.82$, $P^{\dagger} = 0.965$, $\eta^2_p = 0.007$). η^2_p

Contrary to the temporal features, we did not find robust (choice-independent) support for heritability of the spatial features, which describe how connectome states are spatially instantiated in individuals. Specifically, outcomes of equivalent ANCOVAs for $\text{Modularity}_{\text{Time-Varying}}$ ($F_{(3, 337)} = 2.21$, $P^{\dagger} = 0.347$, $\eta^2_p = 0.019$) and $\text{FC}_{\text{Time-Varying}}$ of data-driven clusters ($F_{(3, 337)} = 0.81$, $P^{\dagger} = 1$, $\eta^2_p = 0.007$) showed no impact of sibling status, and effect sizes remained small ($\eta^2_p \sim 0.02$) irrespective of the chosen number of states and GSR (SI Results I, Fig. S3). This lack of robust heritability was confirmed by a subsequent variance-component genetic analysis (see Results III). Our sample size permitted detecting, at 80% power, effects of small size ($\eta^2 = 0.03$, equivalent to $f = 0.179$, or larger). Therefore, if for spatial features heritability produced effects smaller than the detectable size, these effects would be of low practical impact. Further, we provide additional Bayesian Factor values to directly assess the probability of H_0 (i.e., the null hypothesis that there is no effect of sibling status) against H_1 (Table S4). Indeed, the Bayes Factor for $\text{Modularity}_{\text{Time-Varying}}$ showed that the data are more likely to occur under H_0 than under H_1 (BF_{01} of 2.15; anecdotal evidence for H_0). For $\text{FC}_{\text{Time-Varying}}$ of data-driven clusters ($BF_{01} = 131.88$), the Bayes Factor showed that the data are 132 times more likely to occur under H_0 than under H_1.

To ensure that the lack of a robust outcome for spatial attributes was not driven by a narrow feature selection, we further performed additional ANCOVAs of sibling status for exploratory spatial features: $\text{FC}_{\text{Time-Varying}}$ of data-driven clusters defined across four other connection densities (Fig. S4 and Table S5) and $\text{FC}_{\text{Time-Varying}}$ of all 28 possible pairs among the seven ICNs (including within-network FC Tables S6 –7). As with the previous features, we argued that robust heritability effects would persist irrespective of core methodological choices of number of states ($K = 4$ or 6) and GSR/non-GSR. We thus investigated each of the 28 ICN pairs under all four methodological choices. Only a single ICN pair, namely Limbic-Limbic or the set of connections within the Limbic ICN, showed a significant effect of sibling status (corrected for 28 comparisons). This effect was observed for $K = 4$ both under GSR and non-GSR conditions but did not replicate for $K = 6$. For all other exploratory spatial features BF provided anecdotal to decisive evidence for H_0, i.e., the lack of heritability, with exception of three cases under all four methodological choices combined (Tables S5-S7). These findings strongly contrast the observations for temporal features, where Bayes Factor of both Fractional Occupancy and Transition Probability showed that the data are > 100 times more likely to occur under H_1 than under H_0 ($BF_{01} < 10^{-6}$).

Importantly, the effect size of heritability of Fractional Occupancy and Transition Probability was considerably larger for *multivariate* temporal features (Fig. 3) compared to the *individual* (i.e., state-by-state) components of the multivariate features (Table S8). Therefore, our findings demonstrate that the dynamic trajectory of connectome state

transitions are heritable predominantly when considered as multivariate patterns, rather than as individual state-specific components.

3.3. Genetic effects account for substantial variability in temporal connectome dynamics

We employed a structural equation modeling common in classical twin studies (Falconer 1990) to estimate how much of the phenotypic variance is explained by genetic variance, or heritability (h^2). Traditionally, the model is fitted to univariate phenotypes. However, our above-described ANCOVAs suggest that temporal characteristics of connectome dynamics are inherited predominantly as *multivariate* phenotypes (Fig. 3A). Therefore, we adjusted the model to accommodate multivariate phenotypes by quantifying the similarity (or Euclidean distance) between multivariate features from each subject's real data and a "null " point of origin (from dynamics-free surrogate data Fig. 1). To replicate our results independent of this novel approach, we provide results from an alternative approach for multivariate features (Ge et al., 2016), which however does not account for collinearities among the univariate components (SI Results III and Table S9).

A substantial portion of variance of temporal features was explained by additive genetic variance in the ACE model, adjusted for age and head motion (Table 1). The additive genetic effect (A, or narrow-sense heritability) of Fractional Occupancy and Transition Probability was estimated as $h^2 = 0.39$ (95% confidence interval (CI): [.24, 0.54]) for Fractional Occupancy and $h^2 = 0.43$ (95% CI: [.29, 0.57]) for Transition Probability. Note that the impact of common environment (C) was estimated as zero for both Fractional Occupancy and Transition Probability. For both features, the fitness of the nested models was not significantly better than the full ACE model. These outcomes indicate that genetics contribute substantially to the temporal features of connectome dynamics.

Consistent with the ANCOVA-based heritability findings (Fig. 3B and Fig. S3), the ACE model did not support genetic effects on either spatial feature ($FC_{Time\text{-}Varying}$ of data-driven clusters and $Modularity_{Time\text{-}Varying}$). The h^2 was estimated as 0.27 for $FC_{Time\text{-}Varying}$ of data-driven clusters and 0.05 for $Modularity_{Time\text{-}Varying}$, but with a wide 95% CI crossing zero, supporting the null hypothesis (i.e., there is no evidence for heritability): CI of [−0.01, 0.58] and [−54, 0.63], respectively.

3.4. Temporal phenotypes of the dynamic connectome are associated with cognition

Finally, for the heritable phenotypes of connectome dynamics, we assessed associations with cognitive measures using canonical correlation analysis (CCA) (Smith et al., 2015). CCA was performed on dimensionality-reduced data (three principal components for dynamic connectome phenotypes and four factors for cognitive measures). Among the three linear relationships (modes) of covariation, three modes were significant (against 10,000 permutations, $p < 10^{-4}$) and robust after correcting for age, sex, and head motion (Fig. 4A). Post-hoc correlation between the modes and cognitive factors revealed the contribution of each factor to each mode (Fig. 4B). The most significant mode was defined by negative weights for the "Language " ($r = -0.21$) and "Memory" ($r = -0.18$), followed by "Impulsivity " ($r = -0.15$) and "Cognitive control " ($r = -0.13$). The second significant mode was defined by a positive weight for "Cognitive control " ($r = 0.06$). No significant

contribution from cognitive factors was found for the third mode. Post-hoc analysis further revealed substantial contribution of principal components of dynamic connectome phenotypes to the modes. Together, these findings suggest that temporal phenotypes of the dynamic connectome are linked to cognitive abilities.

4. Discussion

The present interest in time-varying dynamics of the functional connectome is rooted in its impact on cognitive processes that are inherently dynamic (Kucyi et al., 2018), with implications for inter-individual differences in cognitive abilities (Eichenbaum et al., 2020; Nomi et al., 2017). Subject-specific features of connectome reconfigurations are both dynamic and multidimensional —they collectively incorporate patterns from multiple connectome states that evolve over time. However, the growing literature on heritability of connectome features has, for the most part, overlooked the connectome's inherently dynamic and multidimensional character. Thus, we introduce a novel method providing comprehensive heritability assessments of a variety of multidimensional dynamic connectome features, and quantify the genetic effects on these multi-dimensional phenotypes (Table 1). This approach successfully demonstrates that heritability effect size is larger and more robust for multivariate dynamic features (i.e., Fractional Occupancy, Transition Probability; Fig. 2 and Fig. S2) than for state-wise scalar features (cf. example here; Table S8). Taken together, our findings provide strong evidence for a substantial genetic effect on the dynamic trajectory of connectome state transitions that does not extend to the spatial and topological features of connectome states.

Previous studies based on the classical twin designs have found considerable genetic effects on multiple structural and *static* (i.e., time-averaged) functional connectome features of the human brain. For example, heritable features of the structural connectome include size (h^2 = 23–60%) and topography (h^2 = 12–19%) of ICNs (Anderson et al. 2021), and average regional controllability as derived from network control theory (h^2 = 13–64%) (Lee et al. 2020). Regarding the functional connectome, heritability has been established for static FC within canonical neurocognitive ICNs in several studies (h^2 = 13– 36% (Adhikari et al., 2018); h^2 = 45–80% (Ge et al., 2017); (h^2 = 9–28% (Elliott et al., 2019)). Further, genetic effects have been reported for topological properties of the static functional connectome, such as global efficiency (h^2 = 52–62%), mean clustering coefficient (h^2 = 47–59%), small-worldness (h^2 = 51–59%), and modularity (h^2 = 38–59%) (Sinclair et al., 2015). The present multivariate approach represents a significant departure from previous studies which traditionally estimate heritability for univariate connectome features. Time-varying changes measured in a multivariate (cross-state) manner are independent of the time-averaged (static) strength of connectivity. Therefore, the previously observed heritability of static connectivity strength and its spatial pattern does not inform about whether or not *changes* in the connectivity pattern are heritable.

Beyond the above-described studies on structural and static functional connectomes, heritability and quantitative estimation of the genetic impact have been largely unknown for connectome dynamics. To our knowledge, only few dynamic features have undergone heritability analysis, specifically Fractional Occupancy across a set of states and their

binary meta-states (Vidaurre et al., 2017) and variance and mean of dynamic connectivity in/across canonical ICNs (Barber et al., 2021). The current study establishes heritability of a wider hypothesis-driven set of multivariate dynamic connectome phenotypes that encompasses both temporal and spatial dynamic features. The statistical effect sizes of heritability were consistently large across several different methodological choices for temporal characteristics of connectome state transitions (Fractional Occupancy and Transition Probability). Further, we provided the quantitative estimate of additive genetic effect on Fractional Occupancy (h^2 = 39%) and Transition Probability (h^2 = 43%), using the classical twin design (Falconer 1990). This strong heritability is in the range reported above for structural and static FC investigations.

Interestingly, for both Fractional Occupancy and Transition Probability, the effect of common environment was estimated to be zero (Table 1). The twin model assumes that environment affects MZ and DZ twins equally and, thereby, greater phenotypic similarity of MZ twins must be due to their greater genetic similarity. However, such biological assumptions can be violated as both intrauterine and postnatal environments can differ as a function of zygosity (Conley et al., 2013). Therefore, the impact of common environment on the phenotypic variance cannot be estimated with precision. Nonetheless, our estimated values suggest that the common environment is unlikely to have a sizable influence on these phenotypes.

Importantly, we showed that the chosen temporal characteristics of connectome state transitions are linked to cognitive abilities. Recently, the well-established association between cognition and structural (Lee et al. 2020) or static functional connectome features (Cole et al., 2013; Elliott et al., 2019; van den Heuvel and Sporns 2013) has been extended to functional connectome *dynamics* (Eichenbaum et al., 2020; Vidaurre et al., 2017). Our observations further corroborate the association between cognitive abilities and connectome dynamics and extends them to our specific features. Although CCA-derived associations cannot reveal the mechanistic nature of this relationship (Eichenbaum et al., 2020), it has been suggested that connectome dynamics may facilitate cognitive processes that are inherently dynamic in nature (J. R. Cohen 2018). Notably, the association with dynamic *temporal* features, specifically, suggest that subject-specific *trajectories* across connectome states are of importance to cognitive processes, most notably language, memory, and cognitive control. Importantly, our observations further suggest genetic contributions to connectome dynamics that impact cognition. A potential driving force of the heritability of such temporal aspects of connectome dynamics could be variability in (e.g., receptor) genes of modulatory neurotransmitter systems. This possibility is in line with a leading theory suggesting that ascending neuromodulatory input may serve as a primary drive behind connectome dynamics and cognition (Shine et al., 2019; 2019). Therefore, the link between dynamic trajectories of the time-varying connectome and cognitive abilities may suggest that temporal phenotypes are potential endophenotypes for cognitive abilities and therefore suitable candidates for genetic association studies.

In contrast to the temporal features, outcomes for spatial characteristics of connectome states largely supported the null hypothesis of a lack of heritability for an extensive set of features. Specifically, for our initial spatial features of cluster-based $FC_{Time\text{-}Varying}$ and

Modularity$_{\text{Time-Varying}}$, sibling status had no effect on similarity across subjects under any of the methodological choices (number of states and GSR). Lack of heritability was confirmed for cluster-based FC$_{\text{Time-Varying}}$ at additional connection densities. Among an exhaustive exploratory set of 28 ICN pairs, FC$_{\text{Time-Varying}}$ did not show an impact of sibling status under any of the methodological choices with exception of within-network FC$_{\text{Time-Varying}}$ in the Limbic ICN. The heritability effect in the Limbic ICN occurred under both GSR and non-GSR choices but was not robust across the chosen number of states. Nevertheless, this observation provides preliminary indication that the Limbic network might be unique in that the change in its FC pattern across connectome states may be under genetic influence. We speculate that this unique observation may be related to the particularly large representation of sub-cortical areas as this aspect posits a major difference compared to the other ICNs. Because of the limited robustness especially in the context of the exploratory approach, this observation should be interpreted with caution and further investigated in future work.

Note that our investigations of FC spatial patterns from discrete whole-brain connectome states are not to be confused with FC variance derived in a state-unrelated manner and in separately studied ICN pairs (Barber et al., 2021); the latter encapsulates temporal characteristics that are indeed heritable, rather than spatial patterns. In principle, our null result for spatial features may be driven by limited signal-to-noise ratio, limited statistical power, or other factors. However, the weight of evidence suggests that genetic effects primarily contribute to how the connectome *transitions* across different states, rather than the precise way in which the states are spatially instantiated in individuals. We note however, that other non-genetic contributors, including individuals' experience and learning, strongly shape the subject-specific connectome and its state-wise spatial patterns. In line with this notion, exploratory analyses (Table S10) showed that our spatial features, albeit not heritable, were significantly associated with all four cognitive Factors (with major contributions from language, memory, cognitive control, and impulsivity, respectively) conforming with prior literature (Eichenbaum et al., 2020).

Our study is subject to several limitations and methodological considerations. In principle, one might conceive of a scenario where genetic effects impact a mental process or a different neurobiological process that in turn affects connectome dynamics. In such a hypothetical case, we believe that our results would still be of basic and translational value as they would demonstrate that genetic effects contribute –via an indirect route– to inter-individual differences in connectome dynamics. Another consideration is that the available sample size is relatively small for a heritability study. Despite this limitation, the confidence intervals indicate that the sample size was sufficient to establish the genetic effect on Fractional Occupancy and Transition Probability with high confidence. Another limitation is that other spatial features that may be heritable may have been missed in this study. In the supplementary, we reported the absence of heritability of a more exhaustive set of features: FC$_{\text{Time-Varying}}$ of data-driven clusters at different connection densities (Table S5) and FC$_{\text{Time-Varying}}$ of 28 ICN pairs (Tables S6–7). However, larger sample sizes may provide insights into heritability of other spatial dynamic features in the future; our results provide a starting point for explorations of these larger feature sets.

In conclusion, our findings establish that transitions between whole-brain connectome states and the proportion of time spent in each state are heritable and subject to substantial genetic influence. These results also suggest a likely non-genetic origin for inter-individual differences in the spatial layout of connectome states. This evidence adds to previous findings linking heritable *temporal* dynamics of connectome states and cognition (Vidaurre et al., 2017; Eichenbaum et al., 2020) and identifies Transition Probability and Fractional Occupancy in the resting human brain as potential endophenotypes for cognitive abilities. As such, these features may inform investigations into specific, functionally relevant genetic polymorphisms and translate to efficient connectome-based biomarkers.

Supplementary Material

Refer to Web version on PubMed Central for supplementary material.

Acknowledgments

Data were provided by the Human Connectome Project, WU-Minn Consortium (Principal Investigators: David Van Essen and Kamil Ugurbil; 1U54MH091657) funded by the 16 NIH Institutes and Centers that support the NIH Blueprint for Neuroscience Research; and by the McDonnell Center for Systems Neuroscience at Washington University. We would like to thank Jaime Derringer for her insight and interpretation of quantitative genetic modeling results and Lili Sahakyan for her insightful feedback on the manuscript. AA holds an MRC eMedLab Medical Bioinformatics Career Development Fellowship. This work was partly supported by the Medical Research Council (grant number MR/L016311/1). This work was partly supported by the National Institute for Mental Health (1R01MH116226 to Sepideh Sadaghiani).

Data availability

HCP datasets are available via (https://db.humanconnectome.org) and also https://registry.opendata.aws/hcp-openaccess/. HMM codes are publicly available from HMM-MAR (multivariate autoregressive) toolbox (https://github.com/OHBAanalysis/HMMMAR).

References

Adhikari Bhim M., Jahanshad Neda, Shukla Dinesh, Glahn David C., Blangero John, Fox Peter T., Reynolds Richard C., et al. , 2018. Comparison of Heritability Estimates on Resting State FMRI Connectivity Phenotypes Using the ENIGMA Analysis Pipeline. Hum Brain Mapp 39 (12), 4893–4902. doi: 10.1002/hbm.24331. [PubMed: 30052318]

Akaike Hirotugu., 1987. Factor Analysis and AIC. Psychometrika 52 (3), 317–332. doi: 10.1007/BF02294359.

Allen Elena, A., Damaraju Eswar, Plis Sergey, M., Erik B, Eichele Tom, Erhardt, Calhoun Vince D., 2014. In: Tracking Whole-Brain Connectivity Dynamics in the Resting State, 24. Cerebral Cortex, New York, N.Y., pp. 663–676. doi: 10.1093/cercor/bhs3521991.

Anderson Kevin, M., Tian Ge, Kong Ru, Patrick Lauren, M., Spreng R., Nathan, Sabuncu Mert, R., Yeo B.T., Thomas, Holmes Avram J., 2021. Heritability of Individualized Cortical Network Topography. Proc. Natl. Acad. Sci 118 (9). doi:10.1073/pnas.2016271118.

Barber Anita D, Hegarty Catherine E, Lindquist Martin, Karlsgodt Katherine H, 2021. Heritability of Functional Connectivity in Resting State: assessment of the Dynamic Mean, Dynamic Variance, and Static Connectivity across Networks. Cereb. Cortex 31 (6), 2834–2844. doi: 10.1093/cercor/bhaa391. [PubMed: 33429433]

Barch Deanna M., Burgess Gregory C., Harms Michael P., Petersen Steven E., Schlaggar Bradley L., Corbetta Maurizio, Glasser Matthew F., et al. , 2013. Function in the Human Connectome: task-FMRI and Individual Differences in Behavior. Neuroimage 80, 169–189. doi: 10.1016/j.neuroimage.2013.05.033. [PubMed: 23684877]

Beckmann Christian F., Smith Stephen M., 2004. Probabilistic Independent Component Analysis for Functional Magnetic Resonance Imaging. IEEE Trans Med Imaging 23 (2), 137–152. doi: 10.1109/TMI.2003.822821. [PubMed: 14964560]

Betzel Richard F., Fukushima Makoto, He Ye, Zuo Xi-Nian, Sporns Olaf, 2016. Dynamic Fluctuations Coincide with Periods of High and Low Modularity in Resting-State Functional Brain Networks. Neuroimage 127, 287–297. doi: 10.1016/j.neuroimage.2015.12.001. [PubMed: 26687667]

Cohen J, 1988. Statistical Power Analysis For the Social Sciences, 2nd ed. Lawrence Erlbaum Associates, Hillsdale, New Jersey.

Cohen Jessica R., 2018. The Behavioral and Cognitive Relevance of Time-Varying, Dynamic Changes in Functional Connectivity. Neuroimage 180 (Pt B), 515–525. doi:10.1016/j.neuroimage.2017.09.036. [PubMed: 28942061]

Cohen Jessica R., D'Esposito Mark, 2016. The Segregation and Integration of Distinct Brain Networks and Their Relationship to Cognition. J. Neurosci 36 (48), 12083– 12094. doi:10.1523/JNEUROSCI.2965-15.2016. [PubMed: 27903719]

Colclough Giles L., Smith Stephen M., Nichols Thomas E., Winkler Anderson M., Sotiropoulos Stamatios N., Glasser Matthew F., Essen David C.Van, Woolrich Mark W., 2017. The Heritability of Multi-Modal Connectivity in Human Brain Activity. Elife 6. doi:10.7554/eLife.20178.

Cole Michael W., Reynolds Jeremy R., Power Jonathan D., Repovs Grega, Anticevic Alan, Braver Todd S., 2013. Multi-Task Connectivity Reveals Flexible Hubs for Adaptive Task Control. Nat. Neurosci 16 (9), 1348–1355. doi:10.1038/nn.3470. [PubMed: 23892552]

Conley Dalton, Rauscher Emily, Dawes Christopher, Magnusson Patrik K.E., Siegal Mark L., 2013. Heritability and the Equal Environments Assumption: evidence from Multiple Samples of Misclassified Twins. Behav. Genet 43 (5), 415–426. doi: 10.1007/s10519-013-9602-1. [PubMed: 23903437]

Douw Linda, Wakeman Daniel G., Tanaka Naoaki, Liu Hesheng, Stufflebeam Steven M., 2016. State-Dependent Variability of Dynamic Functional Connectivity between Frontoparietal and Default Networks Relates to Cognitive Flexibility. Neuroscience 339, 12–21. doi: 10.1016/j.neuroscience.2016.09.034. [PubMed: 27687802]

Eichenbaum Adam, Pappas Ioannis, Lurie Daniel, Cohen Jessica R., D'Esposito Mark, 2020. Differential Contributions of Static and Time-Varying Functional Connectivity to Human Behavior. Network Neuroscience 1–21. doi: 10.1162/netn_a_00172 [PubMed: 32043042]

Elliott Maxwell L., Knodt Annchen R., Cooke Megan, Justin Kim M, Melzer Tracy R., Keenan Ross, Ireland David, et al. , 2019. General Functional Connectivity: shared Features of Resting-State and Task FMRI Drive Reliable and Heritable Individual Differences in Functional Brain Networks. Neuroimage 189, 516–532. doi:10.1016/j.neuroimage.2019.01.068. [PubMed: 30708106]

Falconer DS, 1990. Introduction to Quantitative Genetics. 3rd ed. Longman Group, Harlow, Essex, UK/New York.

Finc K, Bonna K, Lewandowska M, Wolak T, Nikadon J, Dreszer J, Duch W, Kühn S, 2017. Transition of the Functional Brain Network Related to Increasing Cognitive Demands. Hum. Brain Mapp 3, e17.

Finn Emily S., Shen Xilin, Scheinost Dustin, Rosenberg Monica D., Huang Jessica, Chun Marvin M., Papademetris Xenophon, Constable R.Todd, 2015. Functional Connectome Fingerprinting: identifying Individuals Based on Patterns of Brain Connectivity. Nat. Neurosci 18 (11), 1664–1671. doi: 10.1038/nn.4135. [PubMed: 26457551]

Fischl Bruce., 2012. FreeSurfer. Neuroimage 62 (2), 774–781. doi:10.1016/j.neuroimage.2012.01.021. [PubMed: 22248573]

Ge Tian, Holmes Avram J., Buckner Randy L., Smoller Jordan W., Sabuncu Mert R., 2017. Heritability Analysis with Repeat Measurements and Its Application to Resting-State Functional Connectivity. Proc. Natl. Acad. Sci. U.S.A 114 (21), 5521–5526. doi: 10.1073/pnas.1700765114. [PubMed: 28484032]

Ge Tian, Reuter Martin, Winkler Anderson M., Holmes Avram J., Lee Phil H., Tirrell Lee Roffman S, Joshua L, Buckner Randy L., Smoller Jordan W., Sabuncu Mert R., 2016. Multidimensional Heritability Analysis of Neuroanatomical Shape. Nat Commun 7, 13291. doi: 10.1038/ncomms13291. [PubMed: 27845344]

Glahn DC, Winkler AM, Kochunov P, Almasy L, Duggirala R, Carless MA, Curran JC, et al. , 2010. Genetic Control over the Resting Brain. Proc. Natl. Acad. Sci 107 (3), 1223–1228. doi: 10.1073/pnas.0909969107. [PubMed: 20133824]

Glasser Matthew F., Coalson Timothy S., Robinson Emma C., Hacker Carl D., Harwell John, Yacoub Essa, Ugurbil Kamil, et al. , 2016. A Multi-Modal Parcellation of Human Cerebral Cortex. Nature 536 (7615), 171–178. doi: 10.1038/nature18933 [PubMed: 27437579]

Glasser Matthew F., Sotiropoulos Stamatios N., Anthony Wilson, J., Coalson Timothy S., Fischl Bruce, Andersson Jesper L., Xu Junqian, et al. , 2013. The Minimal Preprocessing Pipelines for the Human Connectome Project. NeuroImage, Mapping the Connectome 80, 105–124. doi: 10.1016/j.neuroimage.2013.04.127. [PubMed: 23668970]

Gratton Caterina, Laumann Timothy O., Nielsen Ashley N., Greene Deanna J., Gordon Evan M., Gilmore Adrian W., Nelson Steven M., et al. , 2018. Functional Brain Networks Are Dominated by Stable Group and Individual Factors, Not Cognitive or Daily Variation. Neuron 98 (2), 439–452. doi: 10.1016/j.neuron.2018.03.035, e5. [PubMed: 29673485]

Griffanti Ludovica, Salimi-Khorshidi Gholamreza, Beckmann Christian F., Auerbach Edward J., Douaud Gwenaëlle, Sexton Claire E., Zsoldos Enikő, et al. , 2014. ICA-Based Artefact Removal and Accelerated FMRI Acquisition for Improved Resting State Network Imaging. Neuroimage 95, 232–247. doi: 10.1016/j.neuroimage.2014.03.034. [PubMed: 24657355]

Han Yanting, Adolphs Ralph, 2020. Estimating the Heritability of Psychological Measures in the Human Connectome Project Dataset. PLoS One 15 (7), e0235860. doi: 10.1371/journal.pone.0235860. [PubMed: 32645058]

Hellyer Peter J., Shanahan Murray, Scott Gregory, Wise Richard J.S., Sharp David J., Leech Robert, 2014. The Control of Global Brain Dynamics: opposing Actions of Frontoparietal Control and Default Mode Networks on Attention. J. Neurosci 34 (2), 451– 461. doi: 10.1523/JNEUROSCI.1853-13.2014. [PubMed: 24403145]

van den Heuvel, Martijn P., Sporns Olaf, 2013. Network Hubs in the Human Brain. Trends in Cognitive Sciences, Special Issue: The Connectome 17 (12), 683–696. doi: 10.1016/j.tics.2013.09.012. [PubMed: 24231140]

Hotelling Harold., 1936. Relations between Two Sets of Variates. Biometrika 28 (3–4), 321–377. doi: 10.1093/biomet/28.3-4.321.

Jalbrzikowski Maria, Liu Fuchen, Foran William, Klei Lambertus, Calabro Finnegan J., Roeder Kathryn, Devlin Bernie, Luna Beatriz, 2020. Functional Connectome Fingerprinting Accuracy in Youths and Adults Is Similar When Examined on the Same Day and 1.5-Years Apart. Hum Brain Mapp doi: 10.1002/hbm.25118.

Jenkinson Mark, Beckmann Christian F., Behrens Timothy E.J., Woolrich Mark W., Smith Stephen M., 2012. FSL. Neuroimage 62 (2), 782–790. doi: 10.1016/j.neuroimage.2011.09.015. [PubMed: 21979382]

Keilholz Shella Dawn, 2014. The Neural Basis of Time-Varying Resting-State Functional Connectivity. Brain Connect 4 (10), 769–779. doi: 10.1089/brain.2014.0250. [PubMed: 24975024]

Keller Matthew C., Coventry William L., 2005. Quantifying and Addressing Parameter Indeterminacy in the Classical Twin Design. Twin Research and Human Genetics: The Official Journal of the International Society for Twin Studies 8 (3), 201–213. doi: 10.1375/1832427054253068. [PubMed: 15989748]

Kucyi Aaron, Tambini Arielle, Sadaghiani Sepideh, Keilholz Shella, Cohen Jessica R., 2018. Spontaneous Cognitive Processes and the Behavioral Validation of Time-Varying Brain Connectivity. Network Neuroscience 2 (4), 397–417. doi: 10.1162/netn_a_00037. [PubMed: 30465033]

Liu Wei, Kohn Nils, Fernández Guillén, 2019. Intersubject Similarity of Personality Is Associated with Intersubject Similarity of Brain Connectivity Patterns. Neuroimage 186, 56–69. doi: 10.1016/j.neuroimage.2018.10.062. [PubMed: 30389630]

Lurie Daniel J., Kessler Daniel, Bassett Danielle S., Betzel Richard F., Breakspear Michael, Kheilholz Shella, Kucyi Aaron, et al. , 2020. Questions and Controversies in the Study of Time-Varying Functional Connectivity in Resting FMRI. Network Neuroscience 4 (1), 30–69. doi: 10.1162/netn_a_00116. [PubMed: 32043043]

Newman MEJ, 2006. Finding Community Structure in Networks Using the Eigenvectors of Matrices. Phys. Rev. E 74 (3), 036104. doi: 10.1103/PhysRevE.74.036104.

Nomi Jason S., Vij Shruti Gopal, Dajani Dina R., Steimke Rosa, Damaraju Eswar, Rachakonda Srinivas, Calhoun Vince D., Uddin Lucina Q., 2017. Chronnectomic Patterns and Neural Flexibility Underlie Executive Function. Neuroimage 147, 861– 871. doi: 10.1016/j.neuroimage.2016.10.026. [PubMed: 27777174]

Ousdal Olga Therese, Kaufmann Tobias, Kolskår Knut, Vik Alexandra, Wehling Eike, Lundervold Astri J., Lundervold Arvid, Westlye Lars T., 2020. Longitudinal Stability of the Brain Functional Connectome Is Associated with Episodic Memory Performance in Aging. Hum Brain Mapp 41 (3), 697–709. doi: 10.1002/hbm.24833. [PubMed: 31652017]

Power Jonathan D., Barnes Kelly A., Snyder Abraham Z., Schlaggar Bradley L., Petersen Steven E., 2012. Spurious but Systematic Correlations in Functional Connectivity MRI Networks Arise from Subject Motion. Neuroimage 59 (3), 2142–2154. doi: 10.1016/j.neuroimage.2011.10.018. [PubMed: 22019881]

Quinn Andrew J., Vidaurre Diego, Abeysuriya Romesh, Becker Robert, Nobre Anna C., Woolrich Mark W., 2018. Task-Evoked Dynamic Network Analysis Through Hidden Markov Modeling. Front Neurosci 12. doi: 10.3389/fnins.2018.00603.

Reineberg Andrew E., Hatoum Alexander S., Hewitt John K., Banich Marie T., Friedman Naomi P., 2020. Genetic and Environmental Influence on the Human Functional Connectome. Cereb. Cortex 30 (4), 2099–2113. doi: 10.1093/cercor/bhz225. [PubMed: 31711120]

Robinson Emma C., Jbabdi Saad, Glasser Matthew F., Andersson Jesper, Burgess Gregory C., Harms Michael P., Smith Stephen M., Essen David C.Van, Jenkinson Mark, 2014. MSM: a New Flexible Framework for Multimodal Surface Matching. Neuroimage 100, 414–426. doi: 10.1016/j.neuroimage.2014.05.069. [PubMed: 24939340]

Rosenberg Monica D., Finn Emily S., Scheinost Dustin, Papademetris Xenophon, Shen Xilin, Constable R.Todd, Chun Marvin M., 2016. A Neuromarker of Sustained Attention from Whole-Brain Functional Connectivity. Nat. Neurosci 19 (1), 165–171. doi: 10.1038/nn.4179. [PubMed: 26595653]

Rubinov Mikail, Sporns Olaf, 2010. Complex Network Measures of Brain Connectivity: uses and Interpretations. NeuroImage, Computational Models of the Brain 52 (3), 1059–1069. doi: 10.1016/j.neuroimage.2009.10.003. [PubMed: 19819337]

Sadaghiani Sepideh, Poline Jean-Baptiste, Kleinschmidt Andreas, D'Esposito Mark, 2015. Ongoing Dynamics in Large-Scale Functional Connectivity Predict Perception. Proc. Natl. Acad. Sci 112 (27), 8463–8468. doi: 10.1073/pnas.1420687112. [PubMed: 26106164]

Salimi-Khorshidi Gholamreza, Douaud Gwenaëlle, Beckmann Christian F., Glasser Matthew F., Griffanti Ludovica, Smith Stephen M., 2014. Automatic Denoising of Functional MRI Data: combining Independent Component Analysis and Hierarchical Fusion of Classifiers. Neuroimage 90, 449–468. doi: 10.1016/j.neuroimage.2013.11.046. [PubMed: 24389422]

Shine James M., Breakspear Michael, Bell Peter T., Martens Kaylena A.Ehgoetz, Shine Richard, Koyejo Oluwasanmi, Sporns Olaf, Poldrack Russell A., 2019. Human Cognition Involves the Dynamic Integration of Neural Activity and Neuromodulatory Systems. Nat. Neurosci 22 (2), 289–296. doi: 10.1038/s41593-018-0312-0. [PubMed: 30664771]

Shine James M., Poldrack Russell A., 2018. Principles of Dynamic Network Reconfiguration across Diverse Brain States. NeuroImage, Brain Connectivity Dynamics 180, 396–405. doi: 10.1016/j.neuroimage.2017.08.010. [PubMed: 28782684]

Shine James M., Bissett Patrick G., Bell Peter T., Koyejo Oluwasanmi, Balsters Joshua H., Gorgolewski Krzysztof J., Moodie Craig A., Poldrack Russell A., 2016. The Dynamics of Functional Brain Networks: integrated Network States during Cognitive Task Performance. Neuron 92 (2), 544–554. doi: 10.1016/j.neuron.2016.09.018. [PubMed: 27693256]

Sinclair Benjamin, Hansell Narelle K., Blokland Gabriëlla A.M., Martin Nicholas G., Thompson Paul M., Breakspear Michael, Zubicaray Greig I.de, Wright Margaret J., McMahon Katie L., 2015. Heritability of the Network Architecture of Intrinsic Brain Functional Connectivity. Neuroimage 121, 243–252. doi: 10.1016/j.neuroimage.2015.07.048. [PubMed: 26226088]

Smith Stephen M., Beckmann Christian F., Andersson Jesper, Auerbach Edward J., Bijsterbosch Janine, Douaud Gwenaëlle, Duff Eugene, et al. , 2013a. Resting-State FMRI in the Human

Connectome Project. Neuroimage 80, 144–168. doi: 10.1016/j.neuroimage.2013.05.039. [PubMed: 23702415]

Smith Stephen M., Nichols Thomas E., Vidaurre Diego, Winkler Anderson M., Behrens Timothy E.J., Glasser Matthew F., Ugurbil Kamil, Barch Deanna M., Essen David C.Van, Miller Karla L., 2015. A Positive-Negative Mode of Population Covariation Links Brain Connectivity, Demographics and Behavior. Nat. Neurosci 18 (11), 1565–1567. doi: 10.1038/nn.4125. [PubMed: 26414616]

Smith Stephen M., Vidaurre Diego, Beckmann Christian F., Glasser Matthew F., Jenkinson Mark, Miller Karla L., Nichols Thomas E., et al. , 2013b. Functional Connectomics from Resting-State FMRI. Trends Cogn. Sci. (Regul. Ed.) 17 (12), 666–682. doi: 10.1016/j.tics.2013.09.016.

Stevner ABA, Vidaurre D, Cabral J, Rapuano K, Nielsen SFV, Tagliazucchi E, Laufs H, et al. , 2019. Discovery of Key Whole-Brain Transitions and Dynamics during Human Wakefulness and Non-REM Sleep. Nat Commun 10 (1), 1035. doi: 10.1038/s41467-019-08934-3. [PubMed: 30833560]

Thompson Garth John, Magnuson Matthew Evan, Merritt Michael Donelyn, Schwarb Hillary, Pan Wen-Ju, McKinley Andrew, Tripp Lloyd D., Schumacher Eric H., Keilholz Shella Dawn, 2013. Short-Time Windows of Correlation between Large-Scale Functional Brain Networks Predict Vigilance Intraindividually and Interindividually. Hum Brain Mapp 34 (12), 3280–3298. doi: 10.1002/hbm.22140. [PubMed: 22736565]

Tibon Roni, Tsvetanov Kamen A., Price Darren, Nesbitt David, Can Cam, Henson Richard, 2021. Transient Neural Network Dynamics in Cognitive Ageing. Neurobiol. Aging 105, 217–228. doi: 10.1016/j.neurobiolaging.2021.01.035. [PubMed: 34118787]

Van Essen David C., Smith Stephen M., Barch Deanna M., Behrens Timothy E.J., Yacoub Essa, Ugurbil Kamil, 2013. The WU-Minn Human Connectome Project: an Overview. Neuroimage 80, 62–79. doi: 10.1016/j.neuroimage.2013..05.041. [PubMed: 23684880]

Vatansever D, Manktelow AE, Sahakian BJ, Menon DK, Stamatakis EA, 2017. Angular Default Mode Network Connectivity across Working Memory Load. Hum Brain Mapp 38 (1), 41–52. doi: 10.1002/hbm.23341. [PubMed: 27489137]

Vidaurre Diego, Abeysuriya Romesh, Becker Robert, Quinn Andrew J., Almagro Alfaro, Fidel Smith, Stephen M, Woolrich Mark W., 2018. Discovering Dynamic Brain Networks from Big Data in Rest and Task. Neuroimage 180, 646–656. doi: 10.1016/j.neuroimage.2017.06.077. [PubMed: 28669905]

Vidaurre Diego, Quinn Andrew J., Baker Adam P., Dupret David, Cantero Tejero, Alvaro Woolrich, Mark W, 2016. Spectrally Resolved Fast Transient Brain States in Electrophysiological Data. Neuroimage 126, 81–95. doi: 10.1016/j.neuroimage.2015.11.047. [PubMed: 26631815]

Vidaurre Diego, Smith Stephen M., Woolrich Mark W., 2017. Brain Network Dynamics Are Hierarchically Organized in Time. Proc. Natl. Acad. Sci. U.S.A 114 (48), 12827– 12832. doi: 10.1073/pnas.1705120114. [PubMed: 29087305]

Wang Hao-Ting, Smallwood Jonathan, Mourao-Miranda Janaina, Xia Cedric Huchuan, Satterthwaite Theodore D., Bassett Danielle S., Bzdok Danilo, 2020. Finding the Needle in a High-Dimensional Haystack: canonical Correlation Analysis for Neuroscientists. Neuroimage 216, 116745. doi: 10.1016/j.neuroimage.2020.116745. [PubMed: 32278095]

Yashin Anatoli I., Iachine Ivan A., 1995. Genetic Analysis of Durations: correlated Frailty Model Applied to Survival of Danish Twins. Genet. Epidemiol 12 (5), 529–538. doi: 10.1002/gepi.1370120510. [PubMed: 8557185]

Yeo B.T.Thomas, Krienen Fenna M., Sepulcre Jorge, Sabuncu Mert R., Lashkari Danial, Hollinshead Marisa, Roffman Joshua L., et al. , 2011. The Organization of the Human Cerebral Cortex Estimated by Intrinsic Functional Connectivity. J. Neurophysiol 106 (3), 1125–1165. doi: 10.1152/jn.00338.2011. [PubMed: 21653723]

Zalesky Andrew, Fornito Alex, Bullmore Edward T., 2010. Network-Based Statistic: identifying Differences in Brain Networks. Neuroimage 53 (4), 1197–1207. doi: 10.1016/j.neuroimage.2010.06.041. [PubMed: 20600983]

Further reading

Karen Hodgson, Poldrack Russell A., Curran Joanne E., Knowles Emma E., Mathias Samuel, Göring Harald H.H., Yao Nailin, et al. , 2017. Shared Genetic Factors Influence Head Motion During MRI and Body Mass Index. Cereb. Cortex 27 (12), 5539–5546. doi: 10.1093/cercor/bhw321. [PubMed: 27744290]

Lee Won Hee, Rodrigue Amanda, Glahn David C., Bassett Danielle S., Frangou Sophia, 2020. Heritability and Cognitive Relevance of Structural Brain Controllability. Cereb. Cortex 30 (5), 3044–3054. doi: 10.1093/cercor/bhz293. [PubMed: 31838501]

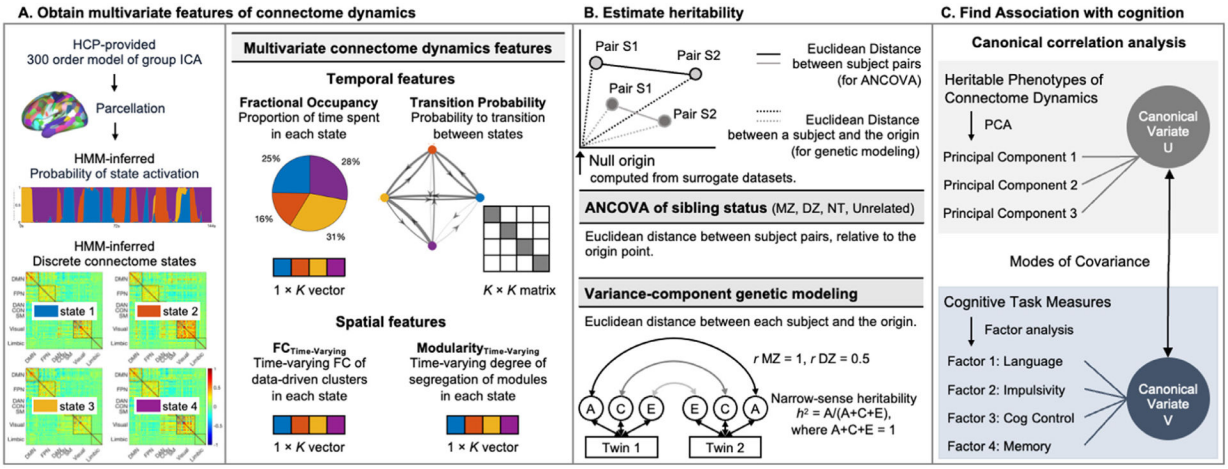

Fig. 1.

An overview of the analysis pipeline. We used minimally preprocessed resting state BOLD timeseries from 139 group-ICA-derived regions covering cortical and subcortical areas of the cerebrum as provided by the Human Connectome Project. [A] We used a hidden Markov model (HMM) to extract K = four discrete connectome states (or K = six states for replication) associated with a state time course for each subject indicating the probability of when each state is active. The four states are color coded (blue, red, yellow, purple) to illustrate their contribution to the connectome dynamics features of interest. We constructed each feature in a multivariate manner to comprehensively represent all states. Multivariate temporal features were defined as the proportion of the recording time spent in each connectome state (Fractional Occupancy) and the probability matrix of transitioning between all possible pairs of discrete states (Transition Probability). Multivariate spatial features include time-varying Modularity ($\text{Modularity}_{\text{Time-Varying}}$), and time-varying connectivity strength ($\text{FC}_{\text{Time-Varying}}$) averaged across the set of connections (region-pairs) that exhibited the strongest dynamic changes across states (Zalesky et al., 2010). [B] We tested whether genetically more related subjects displayed greater similarity in their multivariate features than genetically less related subjects. First, for each feature of dimension m, we estimated a null model-derived origin point in the m-dimensional space. The position of each subject's multi-dimensional feature value was estimated relative to this origin for genetic modeling (see below). Further, the similarity of this position between a given pair of subjects was quantified as Euclidean distance for ANCOVA analyses; a one-way ANCOVA of the factor sibling status with four levels (monozygotic twins (MZ), dizygotic twins (DZ), non-twin siblings (NT), and pairs of unrelated individuals) was performed on the distance value for each of the features. Secondly, we employed structural equation modeling (i.e., genetic variance component model) to quantify the genetic effects. Phenotypic variance of a trait was partitioned into additive genetic (denoted A), common environmental (denoted C) and unique environmental components (denoted E), with narrow-sense heritability (h^2) quantified as the proportion of variance attributed to the genetic factor (A). Path A is dependent on the genetic similarity between twins. MZ twins are genetically identical (path denoted MZ = 1), whereas DZ twins based on the supposition of Mendelian inheritance share half of their genetic information (path denoted DZ = 0.5). [C] Finally, canonical correlation analysis (CCA) was used to find modes of population

covariation between multivariate dynamic connectome features and cognition. CCA analysis was performed on dimension-reduced data including three multivariate dynamic connectome principal components and four cognitive factors.

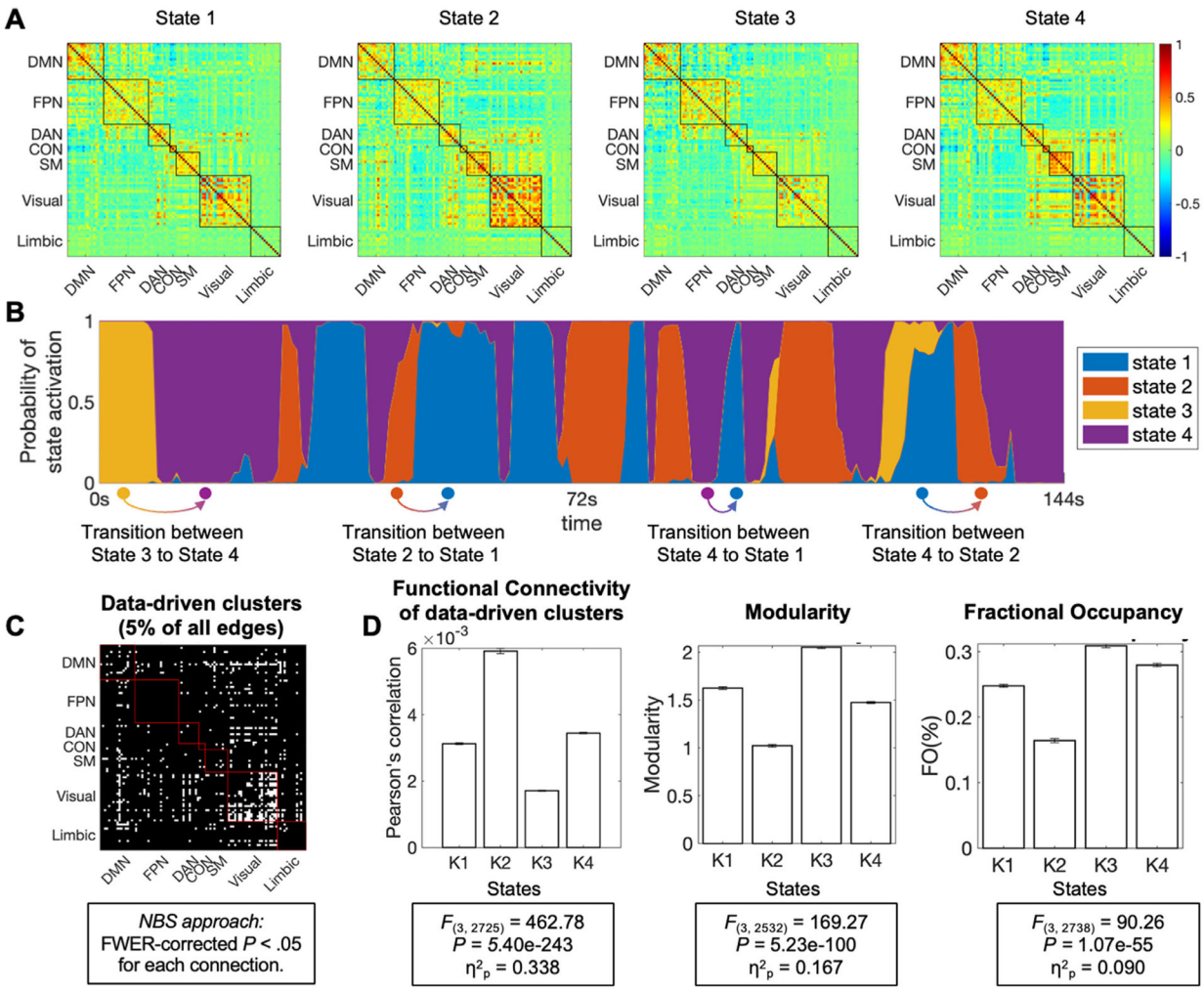

Fig. 2.

HMM states and state-dissociating features. (A) HMM estimates the connectome states that are common to all subjects. The states are represented by z-scored functional connectivity (FC) matrices. The rows and columns represent 139 regions organized according to their membership to canonical intrinsic connectivity networks (ICNs) (Yeo et al., 2011) including default mode network (DMN), frontoparietal network (FPN), dorsal attention network (DAN), salience/cingulo-opercular network (CON), sensory-motor network (SMN), visual network (VIS), and limbic network (Limbic; subcortical limbic regions omitted for visual succinctness). (B) HMM estimates a specific (probabilistic) state time course for each subject indicating when each state is active. The states are characterized by their mean activation and FC matrix. An approximately two-minute section of the state time course is visualized for one subject exemplifying periods occupied by each state and transitions across states. (C) A binary matrix showing a data-driven set of clusters of connections whose FC differed significantly across the four states. *F* values from an connection-wise ANCOVA of FC strength were threshold at 5% connection density followed by Network-Based Statistics (NBS) to control for multiple comparisons (Zalesky et al., 2010). Significant connections are widely distributed across networks, prominently including the DMN and VIS. (D) Bar plots

show the mean FC of data-driven set of clusters, Modularity, and Fractional Occupancy for each state (686 subjects). *F* values are reported for one-way ANCOVAs of the factor state for each variable. Strong differences across states are observed in all three measures. η^2_p: Partial Eta squared effect size. Note that the *F*-tests of the left panel in D is providing equivalent information (and is circular with respect to) the non-parametric test in C. This information is provided solely to facilitate direct comparison with the F-statistics for Modularity and Fractional Occupancy in D. For details, see Fig. S5 and SI Results IV.

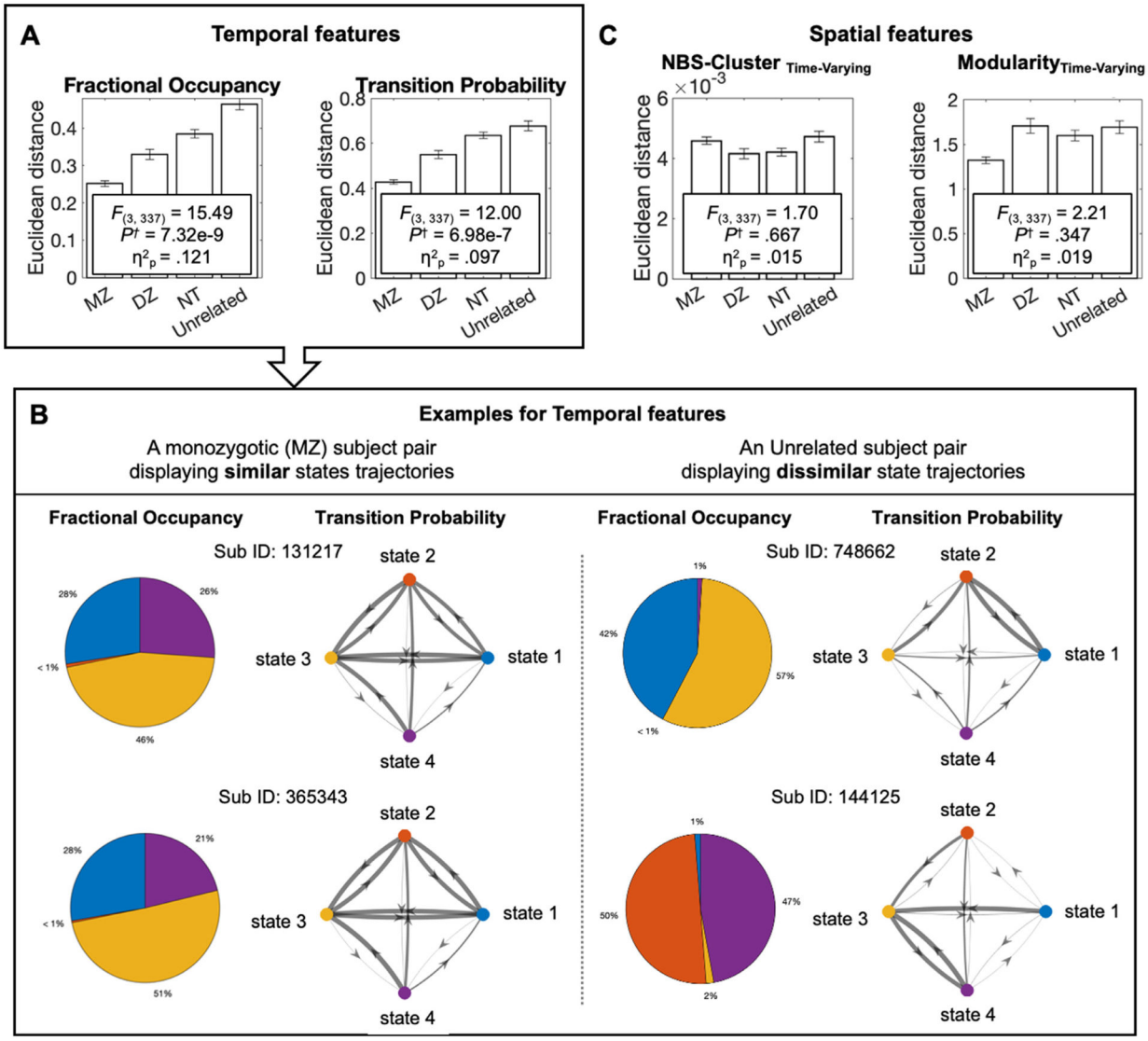

Fig. 3.

Heritability of temporal features of the dynamic connectome. Heritability of each of the multivariate features was assessed separately by one-way ANCOVAs of the factor sibling status (four levels: monozygotic twins (MZ), dizygotic twins (DZ), non-twin siblings (NT), and pairs of unrelated individuals), adjusted for age and head motion. The main effect of sibling status indicates the heritability, or genetic effect. (A) Bar graphs show that more genetically similar subject pairs have smaller Euclidean distance, which denotes similarity of a given temporal connectome feature. Specifically, temporal connectome features were more similar among MZ twin pairs than DZ twins, followed by NT siblings and pairs of unrelated individuals. This heritability effect was statistically significant and stable, irrespective of global signal regression and the chosen number of states (see Fig. S2). (B) The illustration provides an intuition of the similarity of Fractional Occupancy and Transition Probability using the subject pair with highest (*Left*) and respectively lowest (*Right*) multivariate feature similarity. The subject pair in the *Left* panel, an MZ twin set, illustrates that

genetically identical subject pairs display similar duration of time spent in each connectome state (Fractional Occupancy; pie graph) and similar connectome state transition patterns (Transition Probability; directed graph). The subject pair in the *Right* panel were unrelated and illustrate that the temporal features are dissimilar across genetically dissimilar subjects. (C) In contrast to temporal features, bar graphs show that genetic similarity did not affect the similarity of each given spatial connectome features. The effect sizes of the heritability analysis of spatial features remained small for alternative analysis choices (see Fig. S3). $P^{\dagger}$: *P* values Bonferroni-corrected for four dependent variables, $\eta^2_{\ p}$: Partial Eta squared effect size.

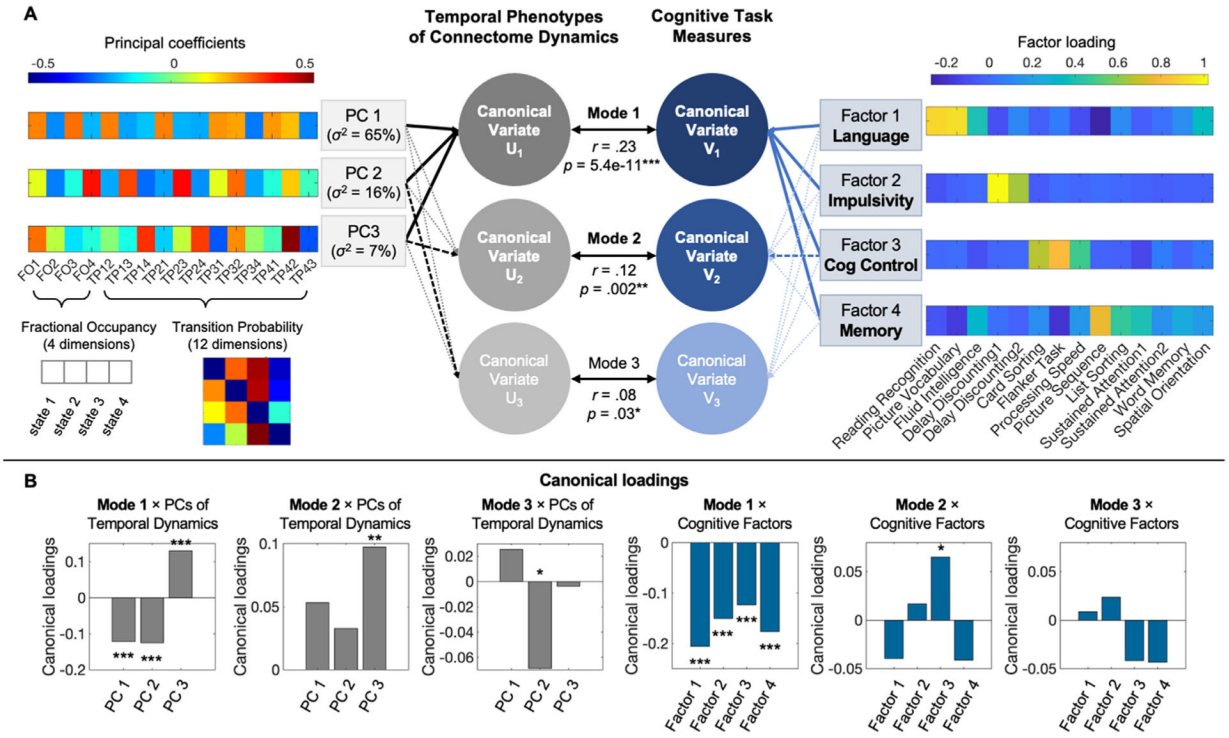

Fig. 4.

Heritable temporal dynamic connectome phenotypes are related to cognition. Canonical correlation analysis (CCA) finds the maximum correlation between the linear combination between the two multi-dimensional canonical variates: U and V. Canonical variate U is defined as the three principal components (PCs), representing the temporal phenotypes of connectome dynamics. Canonical variate V is defined as four Factors, each representing the different domain of cognitive task measures. The principal coefficients matrix displays the weight that each component of the temporal phenotypes has on each of the PCs. The factor loading matrix displays the weight that each cognitive measure has on each of the Factors (see Table S1 for details of cognitive task measures). CCA revealed three significant linear relationships (or modes) between the two canonical variates, corrected for age, sex and head motion. The contribution of each PC or Factor to the given mode (as evaluated through post-hoc Pearson's correlations with each mode) is illustrated by the thickness of the arrows linking PCs or Factors to each canonical variate. These contributions and their statistical significance are quantified by the bar plots in the lower panel. σ^2: the variance explained by each principal component, Cog Control: cognitive control. * $p <$ .05, ** $p <$ .005, *** $p <$ 5.0e-4.

Table 1

Variance-component model parameter estimates of the dynamic connectome features.

Phenotypes	Model	h^2	(95% CI)	A	(95% CI)	C	(95% CI)	E	(95% CI)	−2LL	AIC	χ^2	Δdf	P
Fractional Occupancy	ACE	.39	(0.24, 0.54)	.39	(0.24, 0.54)	.00	(0.0, 0.0)	.61	(0.46, 0.76)	−528.84	−516.84			
	AE	.39	(0.20, 0.51)	.35	(0.20, 0.51)			.65	(0.49, 0.80)	−528.84	−518–84	2.4e–9	1	1.0
	CE					.30	(0.17, 0.43)	.70	(0.57, 0.83)	−525.52	−515.52	3.31	1	.07
Transition Probability	ACE	.43	(0.29, 0.57)	.43	(0.29, 0.57)	.00	(0.0, 0.0)	.57	(0.43, 0.71)	−515.93	−503.93			
	AE	.43	(0.29, 0.57)	.43	(0.29, 0.57)			.57	(0.40, 0.71)	−515.93	−505.93	2.05e–10	1	1.0
	CE					.35	(0.22, 0.47)	.65	(0.53, 0.78)	−512.78	−502.78	3.15	1	.08
$FC_{Time\text{-}Varying}$ of data-driven clusters	ACE	.27	(−0.01, 0.56)	.27	(−0.01, 0.56)	.02	(−0.19, 0.24)	.71	(0.54, 0.87)	−3168.68	−3156.68			
	AE	.30	(0.14, 0.46)	.30	(0.14, 0.46)			.70	(0.54, 0.86)	−3168.67	−3158.67	.009	1	.92
	CE					.23	(0.10, 0.40)	.77	(0.63, 0.90)	−3167.69	−3157.69	.99	1	.32
$Modularity_{Time\text{-}Varying}$	ACE	.05	(−0.54, 0.63)	.05	(−0.54, 0.63)	.07	(−0.36, 0.50)	.88	(0.66, 1.11)	862.05	874.05			
	AE	.14	(−0.06, 0.33)	.14	(−0.06, 0.33)			.86	(0.67, 1.06)	862.15	872.15	.095	1	.76
	CE					.10	(−0.04, 0.24)	.90	(0.76, 1.04)	862.08	872.08	.026	1	.87

All models were adjusted for age and head motion (FD). A, Additive genetic effect; C, common environmental effect; E, Unique/non-shared environment effect; − 2LL, twice the negative log-likelihood; AIC, Akaike's information criterion; df, degrees of freedom; χ^2, chi square, Δdf, change in degree of freedom between the full model and the nested model; *p*, χ^2 test in model fitting. The AE and CE models are nested within the ACE model. Each nested model is compared with the fully saturated model. The fitness of models was tested based on a change in AIC (for a change of df of 1, the statistically significant change in χ^2 is 3.84). h^2, the narrow-sense heritability estimated as $\sigma^2_A/(\sigma^2_A+\sigma^2_C+\sigma^2_E)$; CI: Confidence Interval (lower bound, upper bound); FD, frame-wise displacement.